

# Uncontrolled Manifold Analysis of the Effects of Different Fatigue Locations on Kinematic Coordination During a Repetitive Upper-Limb Task

Matthew Slopecki, Fariba Hasanbarani, Chen Yang,  
Christopher A. Bailey, and Julie N. Côté

Department of Kinesiology and Physical Education, McGill University, Montreal, QC, Canada

Fatigue at individual joints is known to affect interjoint coordination during repetitive multijoint tasks. However, how these coordination adjustments affect overall task stability is unknown. Twelve participants completed a repetitive pointing task at rest and after fatigue of the shoulder, elbow, and trunk. Upper-limb and trunk kinematics were collected. Uncontrolled manifold framework was applied to a kinematic model to link elemental variables to endpoint fingertip position. Mixed and one-way analysis of variances determined effects (phase and fatigue location) on variance components and synergy index, respectively. The shoulder fatigue condition had the greatest impact in causing increases in variance components and a decreased synergy index in the late phase of movement, suggesting more destabilization of the interjoint task caused by shoulder fatigue.

**Keywords:** synergy index, multi-joint task stabilization, compensatory movement, localized joint fatiguing tasks, cyclical pointing movement

Repetitive upper-limb movements are common in workplace tasks and have been associated with pain and musculoskeletal disorders (Punnett & Wegman, 2004). Upper-limb and trunk musculoskeletal disorders were responsible for 53% of 240,682 lost-time claims in Canada in 2016 (Statistics Canada CoC, 2016). Repetitive movements may also lead to fatigue and to the development of upper-limb musculoskeletal disorders over time (Côté, 2014). Fatigue is a disabling symptom comprised of interactions between performance and perceived fatigability (Enoka & Duchateau, 2016). Studies have highlighted coordinated compensation strategies, where individuals adapt their motor patterns to mitigate the development of fatigue (Calvin et al., 2016; McDonald et al., 2019). Studies of repetitive upper-limb tasks have reported


---

Hasanbarani  <https://orcid.org/0000-0002-8050-2275>

Yang  <https://orcid.org/0000-0002-9945-7435>

Bailey  <https://orcid.org/0000-0003-3743-5297>

Côté  <https://orcid.org/0000-0001-6155-8946>

Slopecki (matthew.slopecki@mail.mcgill.ca) is corresponding author,  <https://orcid.org/0000-0001-7134-6023>

changes across multiple joints involved in multijoint tasks (Fuller et al., 2009), and increased magnitude of movement to movement variability in joint angles occurring with fatigue development (Bouffard et al., 2018).

Motor variability is the natural variation in sensorimotor output occurring, to some extent, in all tasks (Srinivasan & Mathiassen, 2012). Motor variability is often quantified at individual joints using simple, unidimensional metrics such as *SD* (Bouffard et al., 2018; Cowley & Gates, 2017; Fedorowich et al., 2013; Srinivasan et al., 2016; Yang et al., 2019). While increased variability has been observed in individual joint angles (Fuller et al., 2011), no changes in intersegmental variability were observed for the fatigued repetitive pointing task (RPT) (Yang et al., 2019). However, they did not analyze how these adaptations impacted task performance, a topic of investigation that can be made using the uncontrolled manifold (UCM) hypothesis.

According to the UCM hypothesis, the system controller acts to reduce the variability of elemental variables (EVs) to a subspace in which the desired outcome of a performance variable (PV) can be achieved. Variability along this subspace,  $V_{UCM}$ , does not affect the PV, meaning this variability is left “uncontrolled.” In contrast, variability orthogonal to this space,  $V_{ORT}$ , that affects task performance, is corrected by the controller (Latash, 2012a). UCM analysis identifies and quantifies synergies, that is, neural organizations that provide low variability (high stability) of a PV by covaried adjustments of EVs (Latash, 2012a). The synergy index ( $\Delta V$ ) is calculated by the relative difference of  $V_{UCM}$  and  $V_{ORT}$ . If  $V_{UCM} > V_{ORT}$ ,  $\Delta V > 0$ , that is, there is a synergy between the EVs that stabilizes the PV. Furthermore, an increase in  $V_{UCM}$  would increase  $\Delta V$ , while an increase in  $V_{ORT}$  would decrease  $\Delta V$  (Latash, 2012a, 2012b). Fisher’s  $z$  transformation is commonly applied to  $\Delta V$  to normalize the data distribution to each participants synergy range, denoted as  $\Delta V_z$  (Zhou et al., 2014).

In upper-limb movement, stabilizing synergies are thought to be developed to preserve a PV linked to the successful completion of a task (Hasanbarani & Latash, 2020; Scholz et al., 2000). UCM analyses have also been used to analyze the effect of fatigue on multielement movement tasks. During multielement finger force production tasks, adaptive increases in force variance components ( $V_{UCM}$  and  $V_{ORT}$ ) by non-fatigued elements were found and interpreted as a strategy to maintain multielement task performance (Park et al., 2012; Singh et al., 2010b), with similar results found in studies when the task was performed in lowly redundant states (Singh et al., 2010a). Increased variance was also found in muscle activations and interpreted as strategies to attenuate effects of fatigue in the lower-limb task (Singh & Latash, 2011). These experimental results provide evidence to support the presence of stabilizing synergies to attenuate the effects of fatigue on task performance. Recently, we used the UCM approach to show that the endpoint coordinates were stabilized both before and after repetitive motion-induced fatigue, although with less stabilizing patterns in the more injury-prone females (Hasanbarani et al., 2021). However, the extent to which these effects were observed due to the presence of actual fatigue in muscles, as opposed to accumulated movement repetitions, remains unknown.

In the workplace, jobs that involve manual material handling may lead to fatiguing different muscles throughout a workday. Studies have shown that fatigue at proximal joints induce higher *SD* during a ratcheting task (Cowley & Gates, 2017). In addition, shoulder fatigue (SF) caused the most significant changes in joint angles displayed during a RPT, compared with trunk fatigue (TF), elbow

fatigue (EF), and no fatigue (NF). Furthermore, SF increased trunk lateral flexion angular variability (Yang et al., 2019). When investigating the variability of continuous relative phase (CRP), the coordination of movement trajectories between two segments (Hamill et al., 1999; Yang et al., 2018, 2019), TF led to a greater trunk–shoulder CRP, implying that trunk movement was delayed relative to shoulder movement, and the trunk–shoulder coordination was adjusted when the trunk muscle was fatigued. Finally, none of the fatigue locations affected CRP variability. However, the impact of these changes on overall task stability, as assessed using the UCM approach, was never verified. Overall, no research to date has investigated the effects of localized fatigue induced on individual joints on the variability and stability characteristics of a repetitive, upper-limb pointing task within the framework of the UCM hypothesis.

Our aim was to assess the effects of fatigue induced using isometric efforts performed until exhaustion in the trunk, shoulder, and elbow regions on variability and stability characteristics of a repetitive upper-limb pointing task. We hypothesized (a) that  $V_{\text{UCM}}$  and  $V_{\text{ORT}}$  would increase in the fatigue conditions, with  $V_{\text{UCM}}$  increasing more than  $V_{\text{ORT}}$ ; (b) that the  $\Delta V$  would increase in the fatigue conditions; and (c) that increased  $V_{\text{UCM}}$  and  $\Delta V_Z$  would be observed when comparing the SF condition to other fatigue locations (Yang et al., 2019). Finally, we hypothesized (d) that differences in  $V_{\text{UCM}}$  and  $\Delta V_Z$  would be found between all conditions (Cowley & Gates, 2017; Yang et al., 2019).

## Methods

### Subjects

Twelve right-handed healthy young adults (five men and seven women, age =  $23 \pm 2.3$  years, height =  $172 \pm 9.6$  cm; body mass =  $63.1 \pm 10.2$  kg), recruited using convenience sampling, participated in the study. Participants were excluded if they had any lower back pain, upper-body injuries, musculoskeletal, or cardiovascular impairments in the 6 months prior to data collection, or if they worked in manual material handling. All participants provided written informed consent prior to participation. The study was approved by the Research Ethics Board of the Center of Interdisciplinary Research in Rehabilitation of Greater Montreal and conducted in accordance with the Helsinki Declaration.

### Experimental Protocol

One 5-s static posture trial was collected before the experimental procedure where participants stood in the anatomical position with arms abducted at  $45^\circ$ . Then, participants completed the RPT. The RPT was performed as outlined in Yang et al. (2019). Briefly, the participant moved their arm repetitively between a proximal and a distal target, aligned at shoulder height along the midline of the participant's body while standing. Proximal and distal targets were placed at 30% and 100% of the participant's arm length, measured from the acromion process to the index fingertip. A movement cadence of 1 Hz per cycle (i.e., one full arm movement forward and backward) was implemented. The touch-sensitive targets provided auditory feedback, allowing participants to synchronize their movement with a

metronome. The participant held a light weight ( $12 \times 7.5 \times 1 \text{ cm}^3$ , 1.4 kg for males, and 0.7 kg for females) during the RPTs to replicate an assembly line task. The participant was familiarized with the RPT before being given a 10-min rest break. Next, the participant performed the RPT for 30 s, recorded as the NF RPT. Ratings of perceived exertion were recorded for the shoulder, triceps brachii, and lower back muscles using the Borg category ratio-10 (CR-10) scale (Borg, 1982) before and after the NF RPT. The participant then completed a series of fatiguing protocols sequentially targeting the muscles of the shoulder, elbow, and trunk (in a random order). Details of the fatiguing protocols can be found in Yang et al. (2019). Briefly, the fatiguing protocols were intermittent static fatiguing tasks, interspersed with 10-s rest periods. The participant gave a Borg CR-10 score for the targeted muscle after each static fatiguing task. The participant repeated each static task until one of two stoppage criteria was met: (a) the participant reached a Borg CR-10 score of 10/10 for the target muscle in three consecutive static trials or (b) the posture could not be maintained for the target time in three consecutive static trials. Participants were unaware of the stoppage criteria. Immediately after each fatiguing task, the participant performed a 30-s RPT as the fatigued RPT (SF, EF, and TF). A 30-min recovery period followed each fatiguing task, where participants sat on a chair and passively recovered (Davidson et al., 2004). Borg CR-10 scores for the target muscles were asked every 5 min. The recovery period continued until the Borg CR-10 score of the target muscle had returned to the pre-NF RPT value.

## Data Acquisition

A seven-camera motion capture system (MX3 VICON, Oxford Metric Ltd.) recorded kinematics at 100 Hz. Fourteen reflective markers (12-mm diameter) were placed on the posterior pelvis; trunk (xiphoid process, seventh cervical vertebra, suprasternal notch, 2 cm to the left and to the right of the eighth thoracic vertebra, LT8 and RT8); upper arm (acromioclavicular joint, medial, and lateral epicondyle); forearm (medial and lateral epicondyle, styloid processes of the radius and ulna); hand (styloid processes of the radius and ulnar, second and fifth metacarpophalangeal joint); and right index finger (second and fifth metacarpophalangeal joint, index fingertip).

## Data Analysis

Kinematic data were processed using Visual 3D (C Motion) then they were filtered (second order, low pass, Butterworth filter, cutoff frequency = 7 Hz, zero phase lag), and joint angles were calculated using a custom MATLAB program (2018) previously described by Hasanbarani et al. (2021). Eleven joint angles at the trunk (abduction–adduction, flexion–extension, and internal–external rotation); shoulder joint (abduction–adduction/horizontal flexion–extension, flexion–extension, and internal–external rotation); elbow joint (flexion–extension); wrist joint (abduction–adduction, flexion–extension, and supination–pronation); and finger (abduction–adduction) were calculated and used as EVs in the subsequent analyses. All angles during the calibration posture were set at 0 radians. The endpoint coordinate (the marker of the index finger) was considered as PV. Only forward reaches were included in the current analyses. Movement time was divided into equal phases of 10%. For statistical analysis, we separated three phases: *Early* (0%–30%), *Middle* (40%–60%), and *Late* (70%–100%).

## UCM Analysis

A forward kinematic model (Hasanbarani & Latash, 2020) was developed to link the changes in the EVs  $\vec{\theta}$  to the PV, the endpoint coordinate ( $x$ ,  $y$ , and  $z$ ). The endpoint coordinates in the 3D space as a function of joint angles  $\vec{\theta}$  is shown in the Appendix.

Partial derivatives of the PV with respect to the EVs (joint angles) were used to form the Jacobian matrix ( $\mathbf{J}$ ). Since the dimension of the PV was three and of the EVs was 11, the matrix dimension is  $3 \times 11$ . The UCM was estimated as the null-space of the corresponding  $\mathbf{J}$  estimated at each movement phase using average trial values of joint angles. The subspace orthogonal to the UCM will be referred to as ORT.

$$\begin{aligned} \mathbf{J}_{\text{Position}}(\vec{\theta}) &= \left[ \frac{\partial P}{\partial \theta_1}, \frac{\partial P}{\partial \theta_2}, \dots, \frac{\partial P}{\partial \theta_9} \right] \\ &= \begin{bmatrix} \partial P_x / \partial \theta_1 & \partial P_x / \partial \theta_2 & \dots & \partial P_x / \partial \theta_{11} \\ \partial P_y / \partial \theta_1 & \partial P_y / \partial \theta_2 & \dots & \partial P_y / \partial \theta_{11} \\ \partial P_z / \partial \theta_1 & \partial P_z / \partial \theta_2 & \dots & \partial P_z / \partial \theta_{11} \end{bmatrix}, \end{aligned} \quad (1)$$

$$\mathbf{J}_{\text{Position}} \times \theta = 0, \quad \text{Space}_{\text{UCM}_{\text{Position}}} = \text{null}[\mathbf{J}_{\text{Position}}].$$

Once the UCM space was computed, we projected the total deviation vector ( $V_{\text{TOT}} = [\vec{\theta} - \vec{\theta}_0]$ ) in the space of EVs onto the UCM (across-trial variance within the UCM is  $V_{\text{UCM}}$ ) and onto the ORT (across-trial variance within the ORT is  $V_{\text{ORT}}$ ):  $V_{\text{ORT}} = V_{\text{TOT}} - V_{\text{UCM}}$ . Finally, the following equations were used to find  $V_{\text{UCM}}$ ,  $V_{\text{ORT}}$ , and  $V_{\text{TOT}}$  over  $N$  trials for each testing setting and for each phase of performance:

$$\begin{aligned} V_{\text{UCM}} &= \frac{\sum_{i=0}^n \overrightarrow{\text{UCM}}_i \cdot \overrightarrow{\text{UCM}}_i}{n \times \text{DOF}_{\text{EV-PV}}}, \quad V_{\text{ORT}} = \frac{\sum_{i=0}^n \overrightarrow{\text{ORT}}_i \cdot \overrightarrow{\text{ORT}}_i}{n \times \text{DOF}_{\text{PV}}}, \\ V_{\text{TOT}} &= \frac{\sum_{i=0}^n \overrightarrow{\text{Total}}_i \cdot \overrightarrow{\text{Total}}_i}{n \times \text{DOF}_{\text{EV}}}, \quad \Delta V = \frac{V_{\text{UCM}} - V_{\text{ORT}}}{V_{\text{TOT}}}, \end{aligned} \quad (2)$$

where  $\overrightarrow{\text{UCM}}_i$  is the total projected vector on the UCM space;  $\overrightarrow{\text{ORT}}_i$  is the total projected vector on the ORT space;  $\Delta V$  represents an index of synergy stabilizing respective the PV; DOF is the number of dimensions in each space, in the current analyses the elemental and PV spaces have 11 and 3 dimensions, respectively. The UCM space is a subspace of the EV space with its dimensions reduced by the number of dimensions of the PVs. In addition, the dimension of the ORT space is limited to the dimension of PV. To eliminate the effect of these dimensions,  $V_{\text{UCM}}$  was divided by  $\text{DOF}_{\text{EV}} - \text{DOF}_{\text{PV}}$ ,  $V_{\text{ORT}}$  by  $\text{DOF}_{\text{PV}}$ , and  $V_{\text{TOT}}$  by  $\text{DOF}_{\text{EV}}$ . Each variance index was normalized by the number of dimensions in the corresponding space. For further statistical analysis, we used Fisher's  $z$  transformation to normalize the data distribution (Zhou et al., 2014).

$$\begin{aligned} \Delta V_{\text{lower}} &= \frac{0 - \frac{V}{\text{DOF}_{\text{PV}}}}{\frac{V}{\text{DOF}_{\text{EV}}}} = -\frac{\text{DOF}_{\text{EV}}}{\text{DOF}_{\text{PV}}}, \quad \Delta V_{\text{upper}} = \frac{\frac{V}{\text{DOF}_{\text{EV-PV}}} - 0}{\frac{V}{\text{DOF}_{\text{EV}}}} = \frac{\text{DOF}_{\text{EV}}}{\text{DOF}_{\text{EV-PV}}}, \\ \Delta V_z &= \frac{1}{2} \left( \ln \left[ \frac{|\Delta V_{\text{lower}}| + \Delta V}{\Delta V_{\text{upper}} - \Delta V} \right] - \ln \left[ \frac{|\Delta V_{\text{lower}}|}{\Delta V_{\text{upper}}} \right] \right), \end{aligned} \quad (3)$$

where  $\Delta V_{\text{upper}}$  is the upper limit of  $\Delta V$  and  $\Delta V_{\text{lower}}$  is the lower limit of  $\Delta V$  (Solnik et al., 2013). Overall, three outcome variables were calculated:  $V_{\text{UCM}}$ ,  $V_{\text{ORT}}$  (variance components, with units of  $[\text{radians}]^2$ ), and  $\Delta V_Z$  ( $\Delta V$ ) for analysis with respect to the endpoint coordinate.

## Statistical Analyses

All data are expressed as mean  $\pm$  SD. Variance data were logarithmically transformed (Yang et al., 2006). Normality of data distribution was tested and confirmed with the Kolmogorov–Smirnov test. A mixed three-way analysis of variance was used to determine the effects of *Phase* (early, middle, and late) and *Fatigue Location* (NF, EF, SF, and TF) on the *Variance Components* ( $V_{\text{UCM}}$  and  $V_{\text{ORT}}$ ). A two-way analysis of variance was used to determine effects of *Phase* (early, middle, and late) and *Fatigue Location* (NF, EF, SF, and TF) on  $\Delta V_Z$ . Pairwise comparisons with Bonferroni corrections were used to report the magnitude of differences for post hoc comparisons. Statistical analyses were conducted in SPSS (version 26) with significance set at  $p < .05$ .

## Results

No significant differences were observed in the average number of trials completed by participants following EF ( $9.3 \pm 4.1$ ), SF ( $8.2 \pm 1.9$ ), and TF ( $9.4 \pm 2.6$ ).

### Variance

Significant main effects of fatigue location:  $F(3, 516) = 5.409$ ;  $p < .01$ ; partial  $\eta^2 = .030$  and phase:  $F(2, 516) = 8.225$ ;  $p < .01$ ; partial  $\eta^2 = .031$ , were observed on the variance data. No interaction effects were found.

Results of the pairwise comparisons for  $V_{\text{UCM}}$  and  $V_{\text{ORT}}$  are displayed in Figures 1 and 2, respectively. Pairwise comparisons revealed that  $V_{\text{UCM}}$  was significantly higher for SF, than for NF ( $0.231 \pm 0.042$ ;  $p < .01$ ), EF ( $0.124 \pm 0.042$ ;  $p < .05$ ), and TF ( $0.166 \pm 0.042$ ;  $p < .01$ ) for  $V_{\text{UCM}}$ .  $V_{\text{UCM}}$  was significantly higher in the early phase, compared with the middle phase ( $0.160 \pm 0.037$ ;  $p < .01$ ) and the late phase ( $0.234 \pm 0.035$ ;  $p < .01$ ). In other words, “good variability” was larger in the RPT post-SF, compared with post-TF or EF, and “good variability” was the lowest in the late phase of the forward movement.

The  $V_{\text{ORT}}$  values were significantly greater in the SF condition, compared with NF ( $0.347 \pm 0.056$ ;  $p < .01$ ), EF ( $0.216 \pm 0.056$ ;  $p < .01$ ), and TF ( $0.253 \pm 0.056$ ;  $p < .01$ ).  $V_{\text{ORT}}$  was also significantly higher in the early phase, compared with the late phase ( $0.131 \pm 0.046$ ;  $p < .05$ ). In other words, similarly to the “good variability,” the “bad variability” during the RPT was the largest after localized SF than after TF or EF, and was largest in the early phase of the forward movement.

### Synergy Index

The  $\Delta V$  was positive in all phases of movement for all conditions, indicating performance-stabilizing strategies. Results of the effects of fatigue on  $\Delta V_Z$  revealed

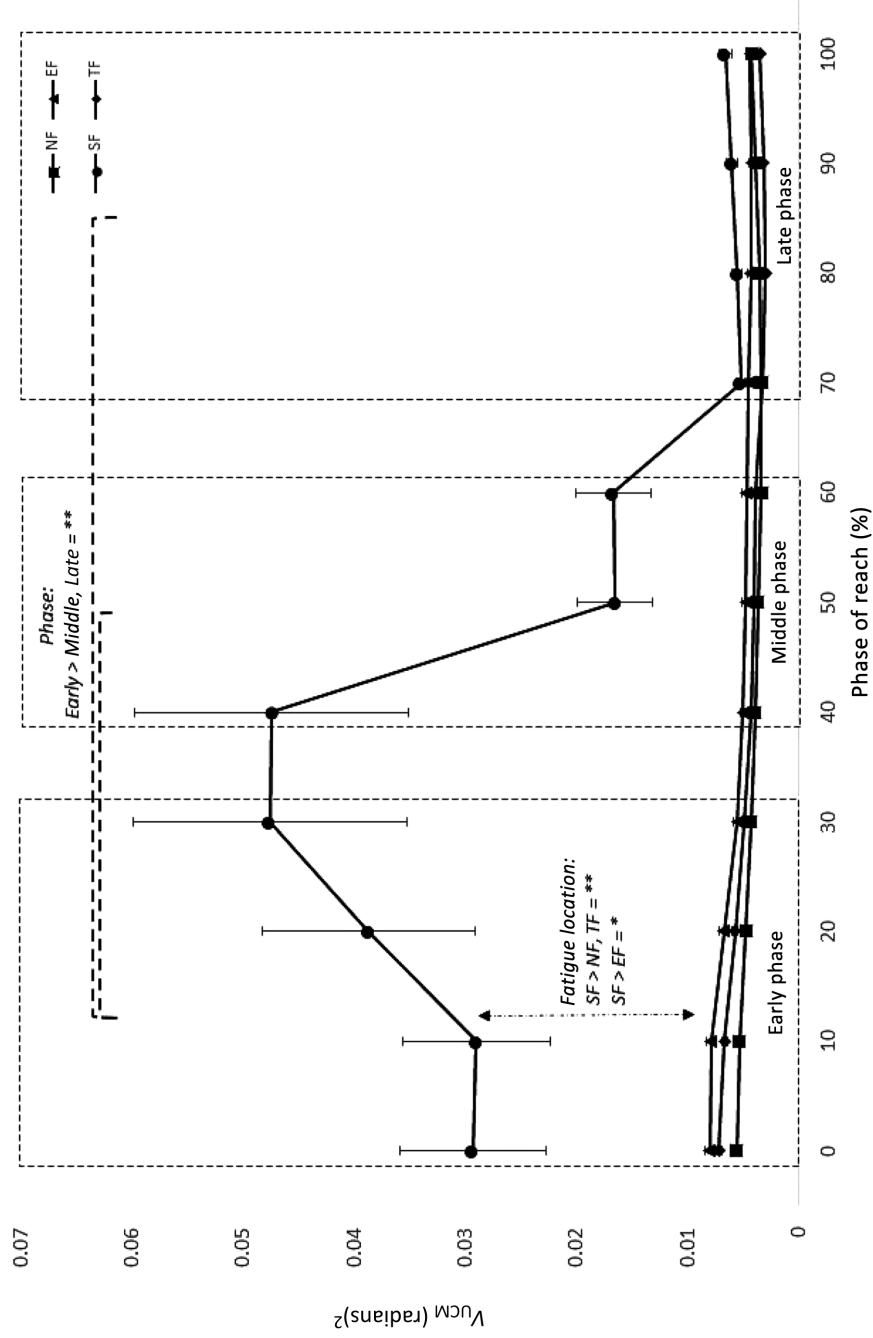


**Figure 1** — Changes in  $V_{UCM}$  (radians)<sup>2</sup> during phases of reach.  $V_{UCM}$  = variability along uncontrolled manifold; TF = trunk fatigue; EF = elbow fatigue; NF = no fatigue; SF = shoulder fatigue. \*Significant pairwise comparison with significance set at  $p < .05$ . \*\*Significant pairwise comparison with significance set at  $p < .01$ .

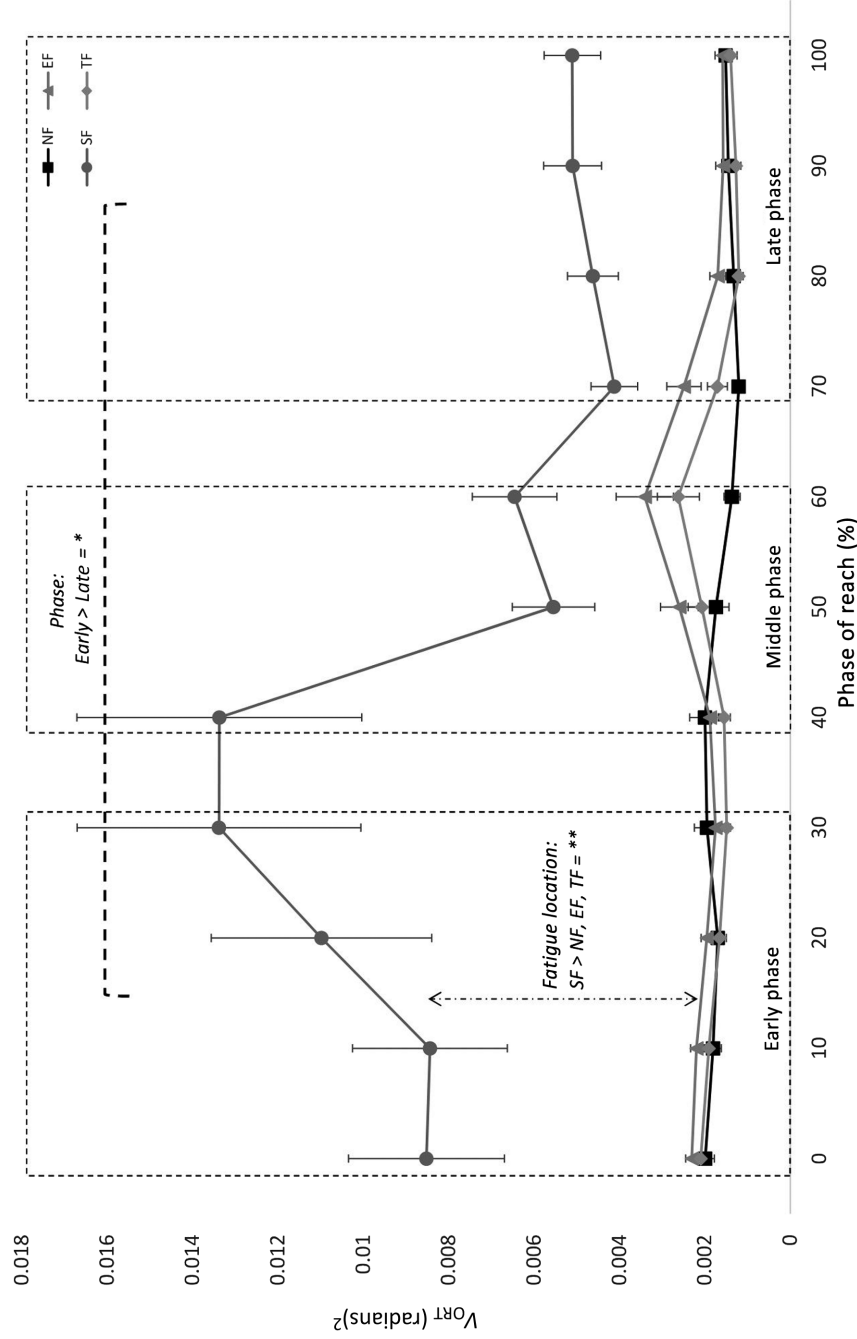


**Figure 2** — Changes in  $V_{ORT}$  (radians)<sup>2</sup> during phases of reach.  $V_{ORT}$  = variability orthogonal; TF = trunk fatigue; EF = elbow fatigue; NF = no fatigue; SF = shoulder fatigue. \*Significant pairwise comparison with significance set at  $p < .05$ . \*\*Significant pairwise comparison with significance set at  $p < .01$ .



significant main effects of fatigue location:  $F(3, 516) = 5.295$ ;  $p < .01$ ; partial  $\eta^2 = .030$  and phase:  $F(2, 516) = 8.134$ ;  $p < 0.01$ ; partial  $\eta^2 = .031$ . No interaction effects were observed.

Results of the pairwise comparisons for  $\Delta V_Z$  are displayed in Figure 3. Pairwise comparisons revealed that  $\Delta V_Z$  was significantly lower (defined as less stable, or more variable) in the SF condition compared with NF ( $-0.131 \pm 0.035$ ;  $p < .01$ ), EF ( $-0.104 \pm 0.035$ ;  $p < .05$ ), and TF ( $-0.099 \pm 0.035$ ;  $p < .05$ ). In other words, fatigue localized to the shoulder joint reduced the stability of the PV to a greater degree than any of the other localized fatigue locations. Also,  $\Delta V_Z$  values were significantly lower in the late phase of movement when compared with early phase ( $-0.117 \pm 0.029$ ;  $p < .01$ ). In other words, the stability of the PV was lower at the end of the forward reach, in comparison to the start.

## Discussion

We analyzed the effects of different fatigue locations on variability of a multijoint task using UCM analysis. We hypothesized (a) that  $V_{UCM}$  and  $V_{ORT}$  would increase in the fatigue conditions, with  $V_{UCM}$  increasing more than  $V_{ORT}$  and (b) that the  $\Delta V$  would increase in the fatigue conditions, as motor variability has been observed as a strategy to adapt to the effects of fatigue to continue performing the RPT (Fuller et al., 2011; Yang et al., 2019). Results show that  $V_{UCM}$  and  $V_{ORT}$  were significantly higher after SF, with relatively higher levels of  $V_{UCM}$  than  $V_{ORT}$ . The  $\Delta V_Z$  was lower in SF than TF and EF conditions. This partly confirmed our hypothesis, as individuals only increased their motor variability after SF. This would suggest that localized fatigue of the elbow and trunk did not inhibit the motor control system from completing the RPT. Moreover, results show that, by far, the destabilizing effects of fatigue on coordination during the RPT were largest after SF, in line with previous findings (Yang et al., 2019) and our third hypothesis. However, our results go a step further in demonstrating that performance of the RPT was stabilized within the UCM space, as shown with a positive  $\Delta V$ , in all fatigue conditions. However, less stability was observed after SF, especially towards the last phase of the forward movement.

## Previous Literature on the RPT

Previous research showed increases in muscle activation magnitudes with fatigue induced by RPT motions especially in the anterior deltoid (Srinivasan et al., 2016), highlighting its role as the prime mover in the RPT. This is consistent with the current findings showing the biggest effect of localized muscle fatigue at the shoulder on the RPT. Localized fatigue has been suggested to reduce the number of movement solutions available, causing a forced reorganization of motor control to maintain task performance (Cowley et al., 2014). The shoulder is in the middle of the trunk–shoulder–elbow kinematic chain. Thus, even though previous results showed that both distal (elbow) and proximal (trunk) fatigue could affect adjacent joints, fatigue at the middle joint (shoulder)-induced changes to both proximal and distal joints (Yang et al., 2019). Moreover, localized SF brought about the biggest overall perturbation to the system. SF changed joint angles of trunk, shoulder and

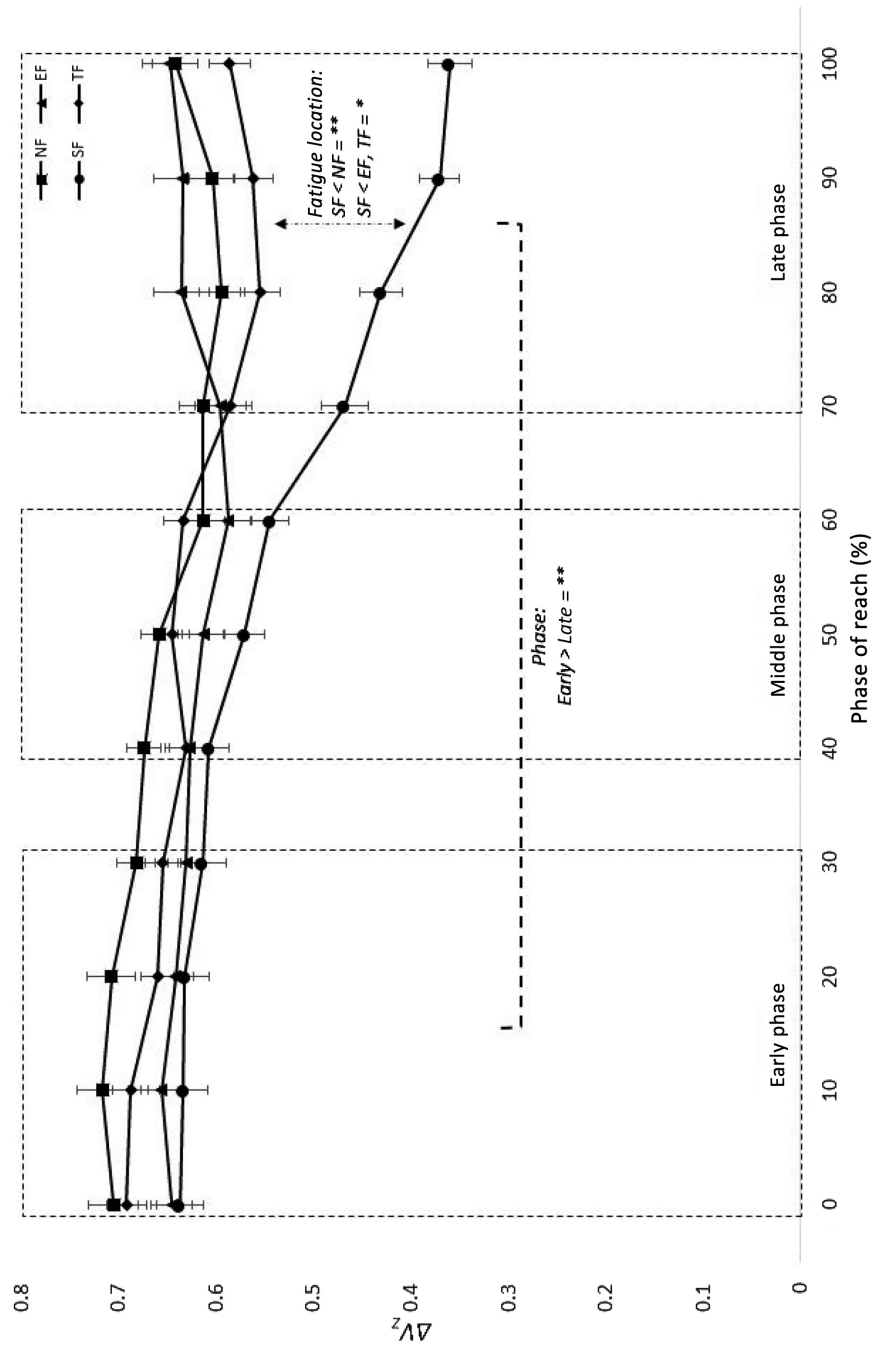


**Figure 3** — Changes in  $\Delta V_z$  during phases of reach.  $\Delta V_z$  = synergy index of Fisher's z-transformation; TF = trunk fatigue; EF = elbow fatigue; NF = no fatigue; SF = shoulder fatigue. \*Significant pairwise comparison with significance set at  $p < .05$ . \*\*Significant pairwise comparison with significance set at  $p < .01$ .

elbow in multiple planes, whereas localized trunk and EF did not change the shoulder angle (Yang et al., 2019). In the present study, this observation is seen through significantly higher  $V_{UCM}$  in the localized SF condition, compared with all other conditions. Localized SF was the only fatigue condition that significantly changed values of the variance components and  $\Delta V$ .

Localized EF changed the mean trunk, shoulder, and elbow angles (Yang et al., 2019). However, it did not change the joint angular variability, multijoint coordination, or the multijoint variability. Localized TF decreased the elbow flexion angle and increased the elbow angle variability. TF also increased the trunk–shoulder coordination. These results implied that localized fatigue at the elbow and trunk affected the joint kinematics from the perspectives of individual joint kinematics. In the present study, localized elbow and TF had negligible effects on the reorganization of motor variability. This further supports the suggestion that localized fatigue of shoulder flexion agonists forced a reorganization of the motor control system to maintain successful task performance. This finding is in opposition to our third hypothesis; differences in  $V_{UCM}$  and  $\Delta V_Z$  would be observed between all fatigue locations.

We also hypothesized that an increased  $V_{UCM}$  and  $\Delta V_Z$  would be observed when comparing the SF condition to other fatigue locations. In the previous analysis of this data set, SF elicited the most significant changes in joint angles and increased trunk lateral flexion angular variability (Yang et al., 2019). However, localized shoulder fatigue did not affect their CRP. A limitation of CRP and *SD* analysis of single joint variability is an inability to study impact on task performance. Addressing this in the present analysis, the shoulder joint was the only fatigue location that elicited higher variance components than at NF. This demonstrates that localized SF increased performance variability, observed as a relative increase of  $V_{ORT}$  to  $V_{UCM}$  in the late phase. Additionally, the elbow and trunk did not require increased compensatory movements at the elemental level to maintain task performance.

### Synergy Reductions in the Late Movement Phase of Localized SF

In the present study, increases in  $V_{UCM}$  and  $V_{ORT}$  and lower  $\Delta V_Z$  were observed in the localized SF condition, compared with all other conditions. A reduced motor synergy was also seen following localized SF. This reduction of  $\Delta V_Z$  at the late phase of reach was the result of a greater decrease in  $V_{UCM}$ , relative to  $V_{ORT}$ . This increased ratio of  $V_{ORT}$  to  $V_{UCM}$  in the late phase represents a more variable task performance. A plausible explanation for this increased task variability in the late phase is due to the increased torque on the fatigued shoulder, as the role of arm weight in fatigue development has been previously outlined (Slopecki et al., 2020). As the arm extends to 100%, the moment arm of the upper limb increases to its maximum, increasing the torque required to maintain arm position and the demand on the motor control system to accurately position the fingertip in space. Another explanation could be the neuromuscular system making anticipatory synergy adjustments (Olafsdottir et al., 2005), manifesting through reductions in synergy stability in preparation to a change in movement direction. In the present study, this would require quickly decelerating the limb to touch the target and begin the backwards movement.

The decrease of  $\Delta V_Z$  in the late phase after localized SF was the result of smaller reductions in  $V_{ORT}$ , relative to  $V_{UCM}$ . This means that, while motor synergies within the UCM space stabilized the PV in the early and middle phases, that is, the endpoint position of the fingertip (Wu & Latash, 2014), task performance was more variable in the late phase after localized SF. This finding is inconsistent with previous literature where endpoint position could be maintained while participants reached a fatigue terminal state (Fuller et al., 2009; Yang et al., 2018). This highlights the importance of the present UCM analyses, as alternative techniques to study movement variabilities were insensitive to this increase in performance variability after SF (Fuller et al., 2009; Yang et al., 2019).

### **Reduction in Variance Components in the Late Movement Phase, Following Localized SF**

In the SF condition,  $V_{UCM}$  and  $V_{ORT}$  were lower in the late phase of movement, compared with the early and middle phases. A potential explanation is that participants are close to a kinematic singularity as the forward movement approaches 100% of the measured arm length. A kinematic singularity occurs when changes in individual joints do not affect the position of the end effector due to a loss of redundancy. However, in the current task, we do not believe that this happened due to the involvement of trunk axial rotation in the RPT. Trunk axial rotation provided the third-largest range of motion for all degrees of freedom measured in the RPT, with  $8^\circ$ – $9^\circ$  reported in conditions of NF (Bouffard et al., 2018). Additionally, the ranges of motion for trunk flexion–extension, lateral flexion, and axial rotation increased with fatigue (Bouffard et al., 2018), even though their  $SD$ s remained constant in the late phases of the RPT (Bouffard et al., 2018). Finally, if a drop in redundancy occurred as the result of the kinematic chain configuration alone, reductions in  $V_{UCM}$  values would be expected in the late phase of all fatigue conditions. However, this reduction is only seen after localized SF. Taken together, this suggests that a kinematic singularity was not reached in the RPT. Individuals were unable to use solutions exclusively within the UCM after localized SF. To continue performance of the RPT, elemental variabilities that affected task performance were used. This highlights the negative effect that localized SF had on motor variability, compared with other fatigue locations in the present study.

### **Individual Differences in Motor Variability Responses to Localized SF**

In the present study, a greater interindividual (i.e. group)  $SD$  was observed following localized SF for both  $V_{UCM}$  and  $V_{ORT}$  values (Figures 1 and 2). This could be due to unique, individualized motor strategies or to common individual features within the group. As such, Hasanbarani et al. (2021) reported that women displayed greater variance component values ( $V_{UCM}$  and  $V_{ORT}$ ), compared with males when fatigued, suggesting sex-specific motor control strategies to mitigate fatigue effects. Thus, the high  $SD$  following localized SF (observed in the present study) may be reflective of sex differences. This is also supported by other studies

displaying sex differences in control of shoulder muscles in the absence and presence of fatigue (Srinivasan et al., 2016). Nevertheless, others have shown no sex differences in several variables relevant to the ones studied here, with one (Bouffard et al., 2018) showing no sex differences in the majority of kinematic variables among a sample of 41 women and 40 men. Thus, we cannot conclude with certainty whether group variability in the measures on our experiment was attributable to sex, which is why, given our small sample size, we elected to not include sex as a variable in the statistical model.

### Limitations

Our sample size was small; thus, sex effects were not investigated. Additionally, kinematic data from other degrees of freedom, such as those at the hip, knee, and ankle, may provide additional information on fatigue-related changes in motor variability linked to task performance.

### Conclusion

Localized SF, compared with other localized fatigue locations and a nonfatigued condition, caused significant increases in  $V_{UCM}$  and  $V_{ORT}$ . Decreased  $\Delta V_Z$  in the late movement phase was observed, particularly following localized SF. This suggests that SF forced greater reorganization in the motor control system to maintain performance of the RPT, although this was reduced following localized SF, specifically during the late phase of movement. This may be due to higher torque exerted on the shoulder joint at late phase of reach, or an anticipatory drop in synergy to facilitate the subsequent backward reach. Future research should incorporate muscle activation variances,  $\Delta V$ , and sex in subsequent analyses.

### References

- Borg, G.A. (1982). Psychophysical bases of perceived exertion. *Medicine & Science in Sports & Exercise*, 14(5), 377–381. <https://doi.org/10.1249/00005768-198205000-00012>
- Bouffard, J., Yang, C., Begon, M., & Côté, J. (2018). Sex differences in kinematic adaptations to muscle fatigue induced by repetitive upper limb movements. *Biology of Sex Differences*, 9(1), 17. <https://doi.org/10.1186/s13293-018-0175-9>
- Calvin, T., McDonald, A.C., & Keir, P.J. (2016). Adaptations to isolated shoulder fatigue during simulated repetitive work. Part I: Fatigue. *Journal of Electromyography and Kinesiology*, 29, 34–41. <https://doi.org/10.1016/j.jelekin.2015.07.003>
- Côté, J.N. (2014). Adaptations to neck/shoulder fatigue and injuries. *Advances in Experimental Medicine and Biology*, 826, 205–228. [https://doi.org/10.1007/978-1-4939-1338-1\\_13](https://doi.org/10.1007/978-1-4939-1338-1_13)
- Cowley, J.C., Dingwell, J.B., & Gates, D.H. (2014). Effects of local and widespread muscle fatigue on movement timing. *Experimental Brain Research*, 232(12), 3939–3948. <https://link.springer.com/content/pdf/10.1007%2Fs00221-014-4020-z.pdf>
- Cowley, J.C., & Gates, D.H. (2017). Proximal and distal muscle fatigue differentially affect movement coordination. *PLoS One*, 12(2), Article e0172835. <https://doi.org/10.1371/journal.pone.0172835>

- Davidson, B.S., Madigan, M.L., & Nussbaum, M.A. (2004). Effects of lumbar extensor fatigue and fatigue rate on postural sway. *European Journal of Applied Physiology*, 93(1–2), 183–189. <https://doi.org/10.1007/s00421-004-1195-1>
- Enoka, R.M., & Duchateau, J. (2016). Translating fatigue to human performance. *Medicine & Science in Sports & Exercise*, 48(11), 2228–2238. <https://doi.org/10.1249/mss.0000000000000929>
- Fedorowich, L., Emery, K., Gervasi, B., & Côté, J.N. (2013). Gender differences in neck/shoulder muscular patterns in response to repetitive motion induced fatigue. *Journal of Electromyography and Kinesiology*, 23(5), 1183–1189. <https://doi.org/10.1016/j.jelekin.2013.06.005>
- Fuller, J.R., Fung, J., & Côté, J.N. (2011). Time-dependent adaptations to posture and movement characteristics during the development of repetitive reaching induced fatigue. *Experimental Brain Research*, 211(1), 133–143. <https://doi.org/10.1007/s00221-011-2661-8>
- Fuller, J.R., Lomond, K.V., Fung, J., & Côté, J.N. (2009). Posture-movement changes following repetitive motion-induced shoulder muscle fatigue. *Journal of Electromyography and Kinesiology*, 19(6), 1043–1052. <https://doi.org/10.1016/j.jelekin.2008.10.009>
- Hamill, J., Van Emmerik, R.E.A., Heiderscheit, B.C., & Li, L. (1999). A dynamical systems approach to lower extremity running injuries. *Clinical Biomechanics*, 14(5), 297–308. [https://doi.org/10.1016/s0268-0033\(98\)90092-4](https://doi.org/10.1016/s0268-0033(98)90092-4)
- Hasanbarani, F., & Latash, M.L. (2020). Performance-stabilizing synergies in a complex motor skill: Analysis based on the uncontrolled manifold hypothesis. *Motor Control*, 24(2), 238–250. <https://doi.org/10.1123/mc.2019-0049>
- Hasanbarani, F., Yang, C., Bailey, C.A., Slopecki, M., & Cote, J.N. (2021). Sex-specific effects of a repetitive fatiguing task on stability: Analysis with Motor Equivalence model. *Journal of Biomechanics*, 129, Article 110769. <https://doi.org/10.1016/j.jbiomech.2021.110769>
- Latash, M.L. (2012a). 9—Coordination. In M.L. Latash (Ed.), *Fundamentals of motor control* (pp. 149–170). Academic Press. <https://doi.org/10.1016/B978-0-12-415956-3.00009-9>
- Latash, M.L. (2012b). The bliss (not the problem) of motor abundance (not redundancy). *Experimental Brain Research*, 217(1), 1–5. <https://doi.org/10.1007/s00221-012-3000-4>
- MATLAB. (2018). *Version 9.5 (R2018b)*. Natick, MA: The MathWorks Inc.
- McDonald, A.C., Mulla, D.M., & Keir, P.J. (2019). Muscular and kinematic adaptations to fatiguing repetitive upper extremity work. *Applied Ergonomics*, 75, 250–256. <https://doi.org/10.1016/j.apergo.2018.11.001>
- Olafsdottir, H., Yoshida, N., Zatsiorsky, V.M., & Latash, M.L. (2005). Anticipatory covariation of finger forces during self-paced and reaction time force production. *Neuroscience Letters*, 381(1), 92–96. <https://doi.org/10.1016/j.neulet.2005.02.003>
- Park, J., Singh, T., Zatsiorsky, V.M., & Latash, M.L. (2012). Optimality versus variability: Effect of fatigue in multi-finger redundant tasks. *Experimental Brain Research*, 216(4), 591–607. <https://doi.org/10.1007/s00221-011-2963-x>
- Punnett, L., & Wegman, D.H. (2004). Work-related musculoskeletal disorders: The epidemiologic evidence and the debate. *Journal of Electromyography and Kinesiology*, 14(1), 13–23. <https://doi.org/10.1016/j.jelekin.2003.09.015>
- Scholz, J.P., Schöner, G., & Latash, M.L. (2000). Identifying the control structure of multijoint coordination during pistol shooting. *Experimental Brain Research*, 135(3), 382–404. <https://doi.org/10.1007/s002210000540>
- Singh, T., & Latash, M.L. (2011). Effects of muscle fatigue on multi-muscle synergies. *Experimental Brain Research*, 214(3), 335–350. <https://doi.org/10.1007/s00221-011-2831-8>

- Singh, T., Varadhan, S.K.M., Zatsiorsky, V.M., & Latash, M.L. (2010a). Adaptive increase in force variance during fatigue in tasks with low redundancy. *Neuroscience Letters*, 485(3), 204–207. <https://doi.org/10.1016/j.neulet.2010.09.012>
- Singh, T., Varadhan, S.K.M., Zatsiorsky, V.M., & Latash, M.L. (2010b). Fatigue and motor redundancy: Adaptive increase in finger force variance in multi-finger tasks. *Journal of Neurophysiology*, 103(6), 2990–3000. <https://doi.org/10.1152/jn.00077.2010>
- Slopecki, M., Messing, K., & Côté, J.N. (2020). Is sex a proxy for mechanical variables during an upper limb repetitive movement task? An investigation of the effects of sex and of anthropometric load on muscle fatigue. *Biology of Sex Differences*, 11(1), 60. <https://doi.org/10.1186/s13293-020-00336-1>
- Solnik, S., Pazin, N., Coelho, C.J., Rosenbaum, D.A., Scholz, J.P., Zatsiorsky, V.M., & Latash, M.L. (2013). End-state comfort and joint configuration variance during reaching. *Experimental Brain Research*, 225(3), 431–442. <https://doi.org/10.1007/s00221-012-3383-2>
- Srinivasan, D., & Mathiassen, S.E. (2012). Motor variability in occupational health and performance. *Clinical Biomechanics*, 27(10), 979–993. <https://doi.org/10.1016/j.clinbiomech.2012.08.007>
- Srinivasan, D., Sinden, K.E., Mathiassen, S.E., & Côté, J.N. (2016). Gender differences in fatigability and muscle activity responses to a short-cycle repetitive task. *European Journal of Applied Physiology*, 116(11–12), 2357–2365. <https://doi.org/10.1007/s00421-016-3487-7>
- Statistics Canada CoC. (2016). *Canadian community health survey (2015–2016)*.
- Wu, Y.-H., & Latash, M.L. (2014). The effects of practice on coordination. *Exercise and Sport Sciences Reviews*, 42(1), 37–42. <https://doi.org/10.1249/jes.0000000000000002>
- Yang, C., Bouffard, J., Srinivasan, D., Ghayourmanesh, S., Cantú, H., Begon, M., & Côté, J.N. (2018). Changes in movement variability and task performance during a fatiguing repetitive pointing task. *Journal of Biomechanics*, 76, 212–219. <https://doi.org/10.1016/j.jbiomech.2018.05.025>
- Yang, C., Leitkam, S., & Côté, J.N. (2019). Effects of different fatigue locations on upper body kinematics and inter-joint coordination in a repetitive pointing task. *PLoS One*, 14(12), Article e0227247. <https://doi.org/10.1371/journal.pone.0227247>
- Yang, J.-F., Scholz, J.P., & Latash, M.L. (2006). The role of kinematic redundancy in adaptation of reaching. *Experimental Brain Research*, 176(1), 54–69. <https://doi.org/10.1007/s00221-006-0602-8>
- Zhou, T., Solnik, S., Wu, Y.-H., & Latash, M.L. (2014). Equifinality and its violations in a redundant system: Control with referent configurations in a multi-joint positional task. *Motor Control*, 18(4), 405–424.

## Appendix: Calculation of the Endpoint Coordinate

$$\begin{aligned}
\text{Position}(\vec{\theta}) = & \text{Pelvis} + L_{\text{TRUNK}} \cdot R_{zx'y''}(\vec{\theta}_{\text{TRUNK}}) \times \vec{D}_0 \\
& + L_{\text{ARM}} \cdot R_{zx'y''}(\vec{\theta}_{\text{ARM}}) \times R_{zx'y''}(\vec{\theta}_{\text{TRUNK}}) \times \vec{D}_0 \\
& + L_{\text{FARM}} \cdot R_z(\vec{\theta}_{\text{FARM}}) \times R_{zx'y''}(\vec{\theta}_{\text{ARM}}) \times R_{zx'y''}(\vec{\theta}_{\text{TRUNK}}) \times \vec{D}_0 \\
& + L_{\text{HAND}} \cdot R_{zx'y''}(\vec{\theta}_{\text{HAND}}) \times R_z(\vec{\theta}_{\text{FARM}}) \times R_{zx'y''}(\vec{\theta}_{\text{ARM}}) \times R_{zx'y''}(\vec{\theta}_{\text{TRUNK}}) \times \vec{D}_0 \\
& + L_{\text{INDEX}} \cdot R_z(\vec{\theta}_{\text{INDEX}}) \times R_{zx'y''}(\vec{\theta}_{\text{HAND}}) \times R_z(\vec{\theta}_{\text{FARM}}) \times R_{zx'y''}(\vec{\theta}_{\text{ARM}}) \\
& \quad \times R_{zx'y''}(\vec{\theta}_{\text{TRUNK}}) \times \vec{D}_0,
\end{aligned} \tag{A1}$$

where Pelvis denotes the coordinates of the posterior pelvis marker,  $L_{\text{TRUNK}}$  is the length of the trunk from pelvis to the right shoulder,  $L_{\text{ARM}}$  is the length of the upper arm,  $L_{\text{FARM}}$  is the length of the forearm,  $L_{\text{HAND}}$  is the length of the hand,  $L_{\text{INDEX}}$  is the length of the index finger, and  $\vec{D}_0$  is a unit vector along the trunk to the shoulder at the point of origin (calibration time).